Article:

Wika, K.K. orcid.org/0000-0001-8422-9416, Litwa, P. and Hitchens, C. orcid.org/0000-0003-1093-0298 (2019) Impact of supercritical carbon dioxide cooling with Minimum Quantity Lubrication on tool wear and surface integrity in the milling of AISI 304L stainless steel. Wear, 426-427 (Part B). pp. 1691-1701. ISSN 0043-1648

https://doi.org/10.1016/j.wear.2019.01.103

Impact of supercritical carbon dioxide cooling with Minimum Quantity Lubrication on tool wear and surface integrity in the milling of AISI 304L stainless steel

Krystian K. Wika*), Przemyslaw Litwa, Carl Hitchens

Nuclear Advanced Manufacturing Research Centre, The University of Sheffield, Brunel Way, Rotherham, S60 5WG, UK

* Corresponding author:

Address: Nuclear Advanced Manufacturing Research Centre, The University of Sheffield, Brunel Way, Rotherham, S60 5WG, UK

Tel. +44 (0)114 222 9900; E-mail address: k.k.wika@sheffield.ac.uk (Krystian K. Wika)

Abstract

In this study, the effect of supercritical carbon dioxide cooling with Minimum Quantity Lubrication ($scCO_2$+MQL) on tool wear and surface integrity of AISI 304L austenitic stainless steel in milling was investigated. A series of machining experiments based on a Design of Experiments (DoE) was carried out at various combinations of cutting parameters to investigate the effect of cutting speed and feed rate on tool wear, near-surface residual stresses, surface roughness and microhardness. The results were compared with the experimental results obtained from milling with flood coolant. A significant improvement in tool life was observed in milling with the $scCO_2$+MQL using multilayer coated tungsten carbide inserts. The tool life in terms of cutting time increased by ~324%, in comparison to a baseline flood coolant. Further, a decrease in surface roughness value (Ra) by about 30%, from 1.09 µm for flood coolant to 0.78 µm after face milling with $scCO_2$+MQL was seen. Additionally, the Ra value slightly increased after machining, for both cooling methods with the increase of cutting speed of ~19%. The observed changes in Ra value were discussed in terms of a built-up-edge (BUE) formation. There were no apparent differences in surface microhardness between both cooling methods. However, the surface microhardness increased with feed rate after milling with both $scCO_2$+MQL and flood coolant due to the increased strain hardening. Also, there was no significant difference in residual stresses after milling, neither with $scCO_2$+MQL nor the flood coolant. The surface residual stress values obtained in the transverse and longitudinal directions were consistent with a predictive model with errors of around 3–8%.

Keywords:

Supercritical carbon dioxide; $scCO_2$; surface integrity; austenitic AISI 304L stainless steel; Minimum Quantity Lubrication (MQL); face milling.

Nomenclature and corresponding units:

a_p	Axial depth of cut, mm
CCF	Central Composite Face design
DF	Degrees of freedom
DoE	Design of Experiments
f_z	Feed rate, mm/tooth
H	Height, mm
L	Length, mm
MLR	Multiple Linear Regression
MQL	Minimum Quantity Lubrication, ml/min
MRV	Material removed volume, cm^3
μHV	Vickers microhardness
φ	Tilt angle, degrees
Q^2	Measure of predictive ability
R^2	Measure of fit
Ra	Arithmetical mean surface roughness value, μm

RSD	Residual Standard Deviation
SEM	Scanning Electron Microscope
$scCO_2$	Supercritical carbon dioxide
VB_{max}	Maximum flank wear, μm
V_c	Cutting speed, m/min
W	Width, mm
XRD	X-Ray Diffraction

1. Introduction

Cutting fluids have been used for decades to facilitate metal removal process, extend tool life, increase productivity in machining processes as well as to improve surface finish and integrity [1–3]. It is well known that orthogonal cutting generates heat by friction and due to plastic deformation in the primary and secondary shear zones [4]. This results in development of high temperature gradients in the cutting zone, leading to rapid tool wear and consequently fracture or catastrophic tool failure [5]. To counter this, there are various cooling techniques used in milling process, such as flood coolant, high pressure coolant, Minimum Quantity Lubrication (MQL) or, more recently, cryogenic cooling with liquid nitrogen or hybrid near-cryogenic cooling techniques, such as carbon dioxide with MQL (CO_2+MQL) [6–8]. From a wide range of parameters influencing tool wear and sufficient performance of a cutting tool, the optimum feed rate and cutting speed when milling are two of the most essential parameters for extended tool life [9]. Optimised cooling conditions can improve surface integrity of a machined surface by supporting a stable growth rate of flank wear in milling processes. The cutting parameters and cooling conditions contribute to the formation of near surface residual stresses, which is accompanied by stress- and deformation-induced martensite formation [10, 11]. This is especially important in machining of metallic components which are exposed to corrosive environments, such as type 304 series stainless steel, widely used in nuclear power plants for steam dryers, primary piping and core structural components [12]. AISI 304 stainless steel is known for having poor machinability due to low thermal conductivity, high ductility and high work hardening rate [13]. Therefore, optimisation of the machining process is required for machinability improvement with longer tool life and to improve machined surface quality. Modern machining processes are typically using soluble oils as cutting fluids [14]. These soluble oils provide lubricity to reduce friction between the cutting tool and machined surface, thus leading to reduction of forces required to remove material and reduce temperature in the cutting zone. A delivery of cutting fluids through the machine tool has seen a trend towards elevated pressures, with 50–70 bar being a standard on the majority of new machine tools aiding in achievement of desired chip breaking. Furthermore, higher pressures (above 150 bar) have started to become a requirement for machining of duplex stainless steel and other difficult to machine materials [15]. These higher pressures are also utilised to further improve the effectiveness of cutting fluids on temperature control. Although the suitability of using the cutting fluids in machining operations have been clearly demonstrated in literature and industrial practice, the financial costs are still significant, with cutting fluids accounting for up to 17% of the overall manufacturing process costs involving the procurement of the cutting fluids, its maintenance and subsequent end of life disposal [16]. In addition, the health and safety risks to the workforce due to direct exposure to these fluids and the mist resulting from high pressure delivery need to be considered. As a result of the limitations of conventional cooling methods, advanced cooling methods or cryogenics have engaged. Most research work on machining with advanced coolants 304 stainless steel refers to turning operations with liquid nitrogen (LN_2) [9]. A limited number of studies on milling of AISI type 304L stainless steel report that cryogenic cooling with LN_2 has no significant advantage over dry milling in terms of tool wear [17]. Some cryogenic cooling strategies have been investigated for environmentally sustainable manufacture (ESM) of metallic components [18, 19]. However, a comparative study between machining of AISI 304 steel using liquid nitrogen (LN_2) and supercritical carbon dioxide ($scCO_2$) has shown that near cryogenic cooling with $scCO_2$ is an effective method to increase the tool life [20]. Pereira et al. established that the use of CO_2+MQL has been shown to improve tool life more than 100% compared to dry machining [20]. In addition, it has been demonstrated that application of the $scCO_2$ cooling in turning of AISI 1045 steel resulted in reduction of cutting forces and tool wear in comparison to use of liquid nitrogen as a coolant [21].

The boiling point of liquid nitrogen and sublimation point of solid CO_2 are -196°C and -79.5°C (at pressure of 1.013 bar) respectively [22, 23]. In addition, the latent heat of sublimation of solid CO_2 (571.1 kJ/kg) is nearly three times higher than that of the latent heat of vaporisation for LN_2 (199 kJ/kg). Therefore, the sublimation of dry ice particles formed by expanding liquid CO_2 through a nozzle (Joule-Thomson effect) allows heat to transfer more efficiently than using liquid nitrogen. Additionally, the solid CO_2 particles can penetrate into the tool-chip interface and transfer heat directly at the surface, as opposed to the liquid nitrogen which transfers heat via a much less effective film boiling process due to the separation of coolant and hot surface by the vapour film [22].

It is also technically easier to retrofit carbon dioxide delivery systems to a standard machine tool, utilising the same existing delivery paths that are used for through-spindle cutting fluids. The necessity for an insulated spindle is also avoided because the $scCO_2$ is transferred through the machine tool at temperatures above 34°C and only at the point of exiting the tool the phase change to a gas and the cooling effects are generated.

Therefore, in this paper $scCO_2$ as an alternative cooling method to LN_2 to reduce the temperature at the cutting tool-chip interface and thus alter the tool life was investigated. The aim of this study was to investigate the effect of the $scCO_2$+MQL cooling on tool wear and surface integrity in the milling of AISI 304L stainless steel. This paper presents a comprehensive analysis of tool life in terms of tool wear (VB_{max}) and material removed volume (MRV). Based upon Design of Experiments (DoE), the relationship between cutting conditions affecting the milling process and the measured output parameters (surface roughness, residual stresses) was analysed. Also, the microhardness and microstructure of the cross-sections from the machined surfaces into the depth of the workpiece material were investigated. The results obtained from milling of AISI 304L stainless steel with the $scCO_2$ as a coolant were compared and contrasted with flood coolant studies at a given set of machining parameters.

2. Materials and methods

2.1 Workpiece materials

Commercially available hot rolled, annealed and pickled austenitic stainless steel 304L plates were used in this experimental work. The experiments were divided into two stages: design of experiment (DoE) and tool life trials. The DoE experiments were performed on flat plates, 110 mm (W) × 190 (L) mm × 30 (H) mm, provided by Jacquet UK Ltd. The tool life trials were conducted on flat plates, 290 mm (W) x 190 mm (L) x 100 mm (H), provided by Kloeckner Metals UK. The chemical compositions of stainless steel 304L plates used in this study are presented in Table 1.

Table 1. Typical chemical composition of austenitic stainless steel 304L.

Plate dimensions (W×L×H) [mm]	Elements (wt.%)								
	C	Si	Mn	P	S	Cr	Ni	N	Co
110×190×30	0.022	0.290	1.720	0.036	0.002	18.14	8.05	0.0919	0.154
290×190×100	0.024	0.310	1.885	0.035	0.0016	18.010	8.036	0.0822	0.158

2.2 Experimental setup and cutting conditions

All experimental work was carried out on a 4-axis Starrag Heckert HEC1800 horizontal milling machine tool with traversing table and a column mounted spindle with a maximum spindle speed of 4000 rpm and torque of 2150 Nm. The machine tool has a Sinumerik 840D controller. The plates used in the DoE experiments were fastened to a Hilma NC160 vice that was vertically fixed to a tombstone block. Fig. 1 shows the experimental setup for climb milling of stainless steel 304L. Prior to the experiments, 30 mm thick stainless steel 304L plates were machined to create two 14 mm wide and 5 mm deep slots as shown in Fig. 1(b). These slots allowed four machining passes to be achieved on each 30 mm thick plate. Tool engagement was kept constant at 80% in both the DoE and tool wear trials.

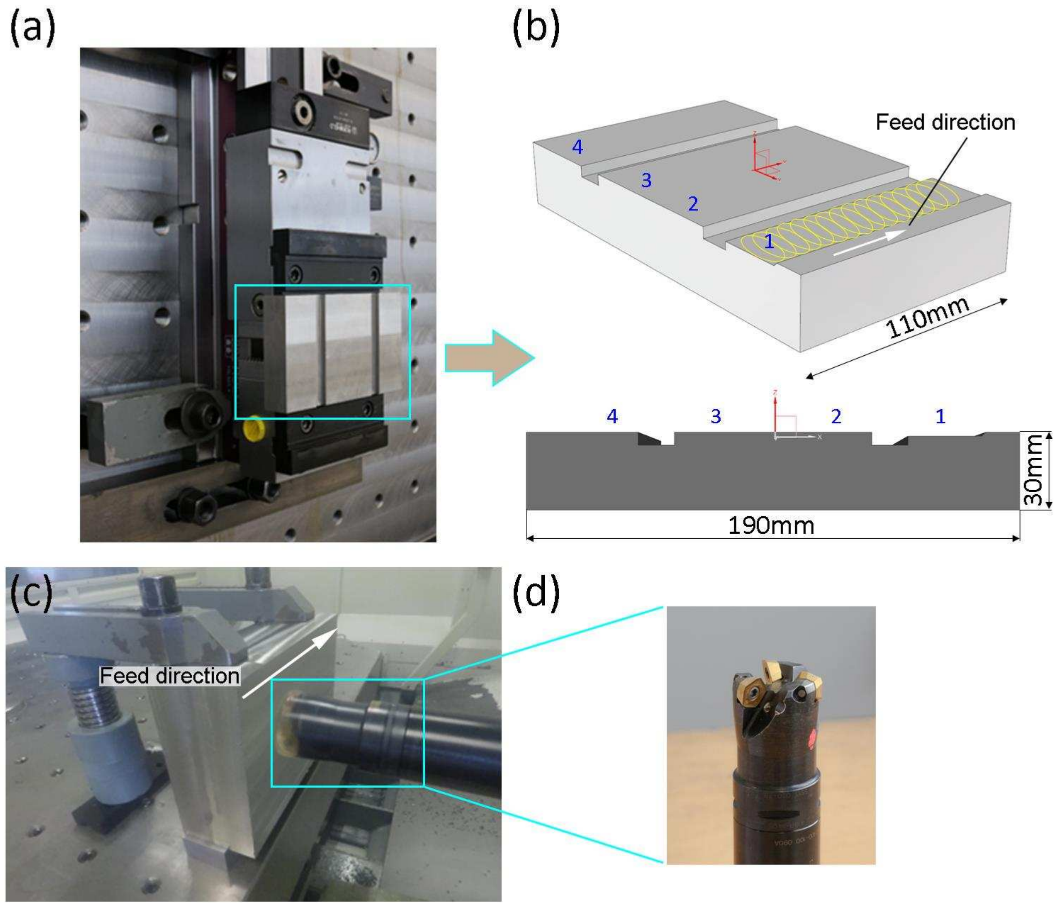

Fig. 1. Machining setup: (a, b) DoE experiments, (c) tool wear trials, (d) cutting tool used in the experiments.

In Fig. 1(b), a single pass is schematically marked with yellow overlapping elliptic shapes. The plate for tool life trials was placed on the machine flat bed and fastened using standard manual end clamps [Fig. 1(c)]. The Starrag HEC1800 was retrofitted with a supercritical carbon dioxide (scCO_2) unit manufactured by Fusion Coolant Systems. The unit provides a fine tuned stream of scCO_2 (with an option to run it with or without MQL). In order to minimise chip adhesion during machining of stainless steel 304L and provide lubrication in the cutting zone, 1 ml/min of soybean oil (NuCut Plus MQL oil) was mixed with the scCO_2. The MQL oil was fully dissolved in the scCO_2 due to the supercritical properties of the CO_2 and the mixture was delivered through the tool.

The cutting tool used in all experimental work was a Ø42 mm 419 series high feed face mill (419-042C4-14M) in C4-390.410-100 holder from Sandvik Coromant (Fig. 1(d)). The tool had three cutting inserts. The 419R-1405E-MM carbide (grade 2040) inserts, coated with $Ti(C,N)+Al_2O_3+TiN$, were used during the experiments. The face milling cutter coolant delivery ports were specially modified to accommodate the 0.25 mm diameter coolant nozzles. The milling cutter had three coolant nozzles and at an operating pressure of around 138 bar, resulted in a CO_2 flow rate of ~39 kg/hour. The flood coolant was delivered at 50 l/min flow rate under the pressure of 6 bar.

2.3 Methods and experimental techniques

The DoE experiments were conducted based on a Central Composite Face (CCF) design. The design was composed of a full factorial design and star points placed on the faces of the sides. This design allowed the detection of quadratic models. An alpha level of 0.05 (5% significance level) was selected as this is a good balance between Type I and Type II errors in hypothesis tests. The experimental work was conducted according to a three-level design with 8 runs in the design, 1 centre point and 1 replicate resulting in total of 18 actual runs. The 18 runs were divided into two blocks to minimise the effect of nuisance factors. Statistical analysis of the data was made with the help of MODDE 12.0.1 software to evaluate the significance of experimental results. The Multiple Linear Regression (MLR) multivariate method was used to construct the predictive models as it deals with and fits one response at a time (based on the assumption that the responses are independent [24]). Table 2 presents the cutting parameters used in the DoE stage of experiments.

Table 2. Cutting conditions used during the DoE experiments.

Factor	Feed rate f_z (mm/tooth)	Cutting speed V_c (m/min)
Low level	0.50	215
Medium level	0.85	235
High level	1.20	255

The tool life trials were conducted according to ISO 8688-1:1989 [25]. Each 290 mm × 190 mm plane allowed up to seven passes with the 42 mm high feed cutter. The cutting passes were taken along the 290 mm long edge with a 1 mm depth of cut.

The residual stresses were determined using a laboratory based X-ray diffraction (LXRD) residual stress measurement system provided by Proto. The Manganese target with Mn K-alpha radiation at a wavelength of 2.10314 Å was used. The X-ray tube has been adjusted to the point focus position using a point aperture slit with a diameter of 2 mm. The stress analysis was carried out based on the $\sin^2\psi$ method using a specific (311) diffraction plane for the austenitic stainless steel [26]. The interplanar spacing (d_{311}) was measured by the X-ray diffraction at different tilt angles (φ), which were defining the orientation of the workpiece surface. The elastic strains were determined from the shift in the interplanar spacing for the (311) reflection caused by milling with the different cutting conditions. The residual stresses were measured in the transverse (φ = 0°) and the longitudinal (φ = 90°) directions using the following isotropic elastic constant values: $s_1 = 1.20\times10^{-6}$ (1/MPa) and $(½)s_2 = 7.18\times10^{-6}$ (1/MPa). After the residual stress measurements, the plates were cut into small pieces, 30 mm (W) × 40 mm (L), for surface roughness measurements and then for microhardness and microstructural analyses. The specimens were cut from the middle of the tool path to avoid a gradual change in cutting forces upon entry and exit of the tool during face milling.

The surface roughness was measured on a KEYENCE VK-X200 series laser microscope according to ISO 4287:1997 [27]. The arithmetical mean roughness value (Ra) was calculated from the roughness profile, which was obtained from the primary profile after λ_c high-pass filtering with a cut-off wavelength of 0.8 mm. The Ra was calculated as the average value from six sampling lengths where the roughness evaluation length was 0.4 mm.

The micro hardness testing was carried out using the TUKON 2500 automated hardness tester under a load of 100 g with a standard dwell time of 15 seconds. The cross-sectional Vickers micro hardness (µHV) was measured on the polished specimens at a depth of 30 µm from the machined surface every 35 µm in depth up to about 400 µm. The micro hardness results are the average values of a three independent measurements (at the same distance from the machined surface). For microstructural analysis, the specimens were polished and electrolytically etched with aqueous oxalic acid. The microstructure of the machined surfaces was studied using the Phenom XL scanning electron microscope (SEM) operating at the backscattered (BSE) electron mode at a beam voltage of 15 kV.

3 Results and discussion

3.1 Tool wear trials in stainless steel 304L face milling

Table 3 summarises the results from eight cutting trials providing cutting parameters and their corresponding tool life and material removed volume (MRV).

Table 3. A summary of tool wear trials and their corresponding tool life.

Trial name	Type of coolant	Cutting parameters		Cutting length (m)	Cutting time (min)	MRV (cm^3)
		f_z (mm/tooth)	V_c (m/min)			
Ex1	Flood	0.50	215	8.12	2.63	216
Ex2	Flood	1.20	215	25.20	3.40	669
Ex3	Flood	0.50	255	16.24	4.43	431
Ex4	Flood	1.20	255	24.36	2.77	647
Ex5	$scCO_2$+MQL	0.50	215	34.51	11.16	917
Ex6	$scCO_2$+MQL	1.20	215	65.10	8.77	1729
Ex7	$scCO_2$+MQL	0.50	255	56.70	15.46	1506
Ex8	$scCO_2$+MQL	1.20	255	50.40	5.73	1339

Fig. 2 shows the impact of different sets of cutting conditions on the flank wear of coated carbide inserts and their resulting tool life.

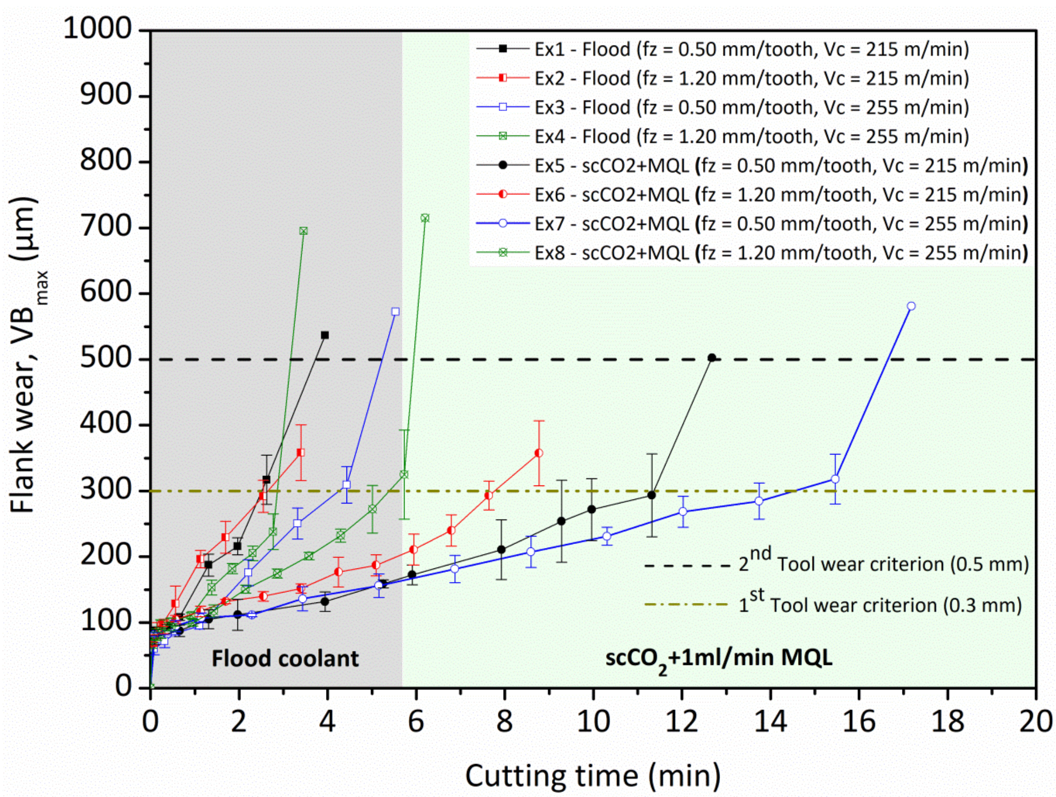

Fig. 2. The maximum flank wear (VB_{max}) values as a mean of three individual cutting edges measurements.

The flank wear was measured on three cutting inserts. The results are presented as a mean of maximum flank wear (VB_{max}) of all three inserts using a 300 µm as the first tool wear criterion determined from the acceptance and 500 µm as the second tool wear criterion. The trials were terminated when at least one of the cutting inserts exceeded the second criterion.

In this tool life study, the feed rate, cutting speed and cooling method were varied while the depth of cut and tool engagement were kept constant. For any set of cutting conditions tool life achieved with the assistance of the $scCO_2$ far exceeded the one with flood coolant. Fig. 2 indicates that generally with an increase in feed rate (from 0.5 to 1.20 mm/tooth at constant cutting speed and cooling method), the tool life in terms of cutting time decreased.

An increase in tool life when the cutting speed increased from 215 to 255 m/min was seen only at low feed rate (0.5 mm/tooth). At the higher feed rate (1.2 mm/tooth), the opposite phenomena was observed, i.e. with an increase in cutting speed, the tool life decreased.

The highest tool life of 15.46 minutes was observed with the $scCO_2$ (V_c = 255 m/min; f_z = 0.5 mm/tooth) in comparison to 4.43 minutes for flood coolant (an increase of 249%). On the other hand, the highest increase in tool life of ~324% was seen with the assistance of the $scCO_2$ (11.16 minutes) in comparison to only 2.63 minutes in the case of flood coolant (V_c = 215 m/min and f_z = 0.5 mm/tooth). Excessive chipping was observed (regardless of cooling conditions) at higher cutting speeds and feeds due to higher cutting forces and resulted in a weaker cutting edge. Also, the growth of wear on the flank face was more uniform at the higher cutting speed and lower feed rate of 0.50 mm/tooth due to low vibrations. Typically, with an increase in cutting speed and decrease in feed rate, the vibrations decreased [28]. Therefore, higher cutting speed and lower feed rate resulted in an increased tool life and the growth rate of flank wear was more stable in comparison to milling at high feed rate. Comparing the cooling efficiency, milling with the $scCO_2$+MQL shows a tendency towards longer tool life in comparison to a baseline flood coolant. A combination of high cutting speed and low feed rate yielded the highest improvement in tool life. As regards the tool life measured in machined distance, the highest results were obtained with the $scCO_2$+MQL (65.1 m), whereas the flood coolant yielded 25.2 m (1.2 mm/tooth and 215 m/min). Fig. 3 shows the flank wear (VB_{max}) as a function of removed volume of material using 300 µm flank wear criterion.

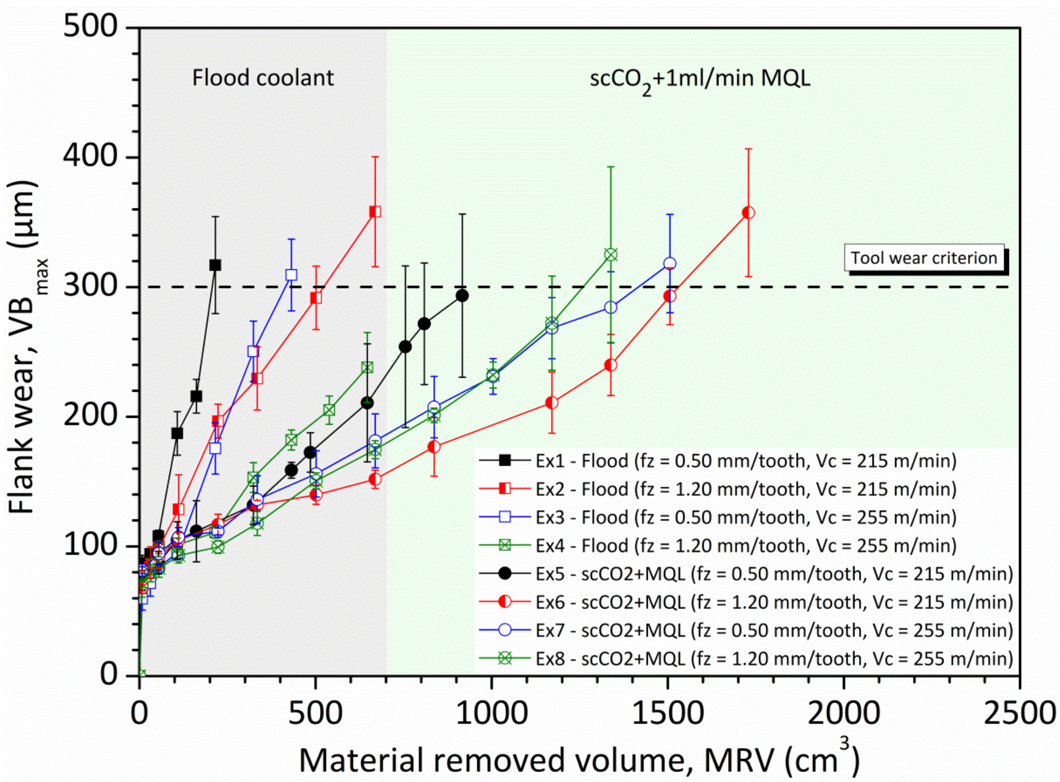

Fig. 3. Flank wear (VB_{max}) as a function of material removed volume.

From Table 3 and Fig. 3, the highest observed material removed volume (MRV) was 1729 cm^3 in milling with the $scCO_2$ (f_z = 1.20 mm/tooth and V_c = 215 m/min. This is ~158% improvement in the MRV using $scCO_2$ in contrast to milling with flood coolant (669 cm^3). When milling with the assistance of $scCO_2$, a cutting speed of 215 m/min and feed rate increasing from 0.5 to 1.2 mm/tooth it was seen that both tool life and the material removed volume increased (Table 3).

Fig. 4(a) shows a comparison analysis between tool life and the volume of material removed when milling with flood coolant and $scCO_2$.

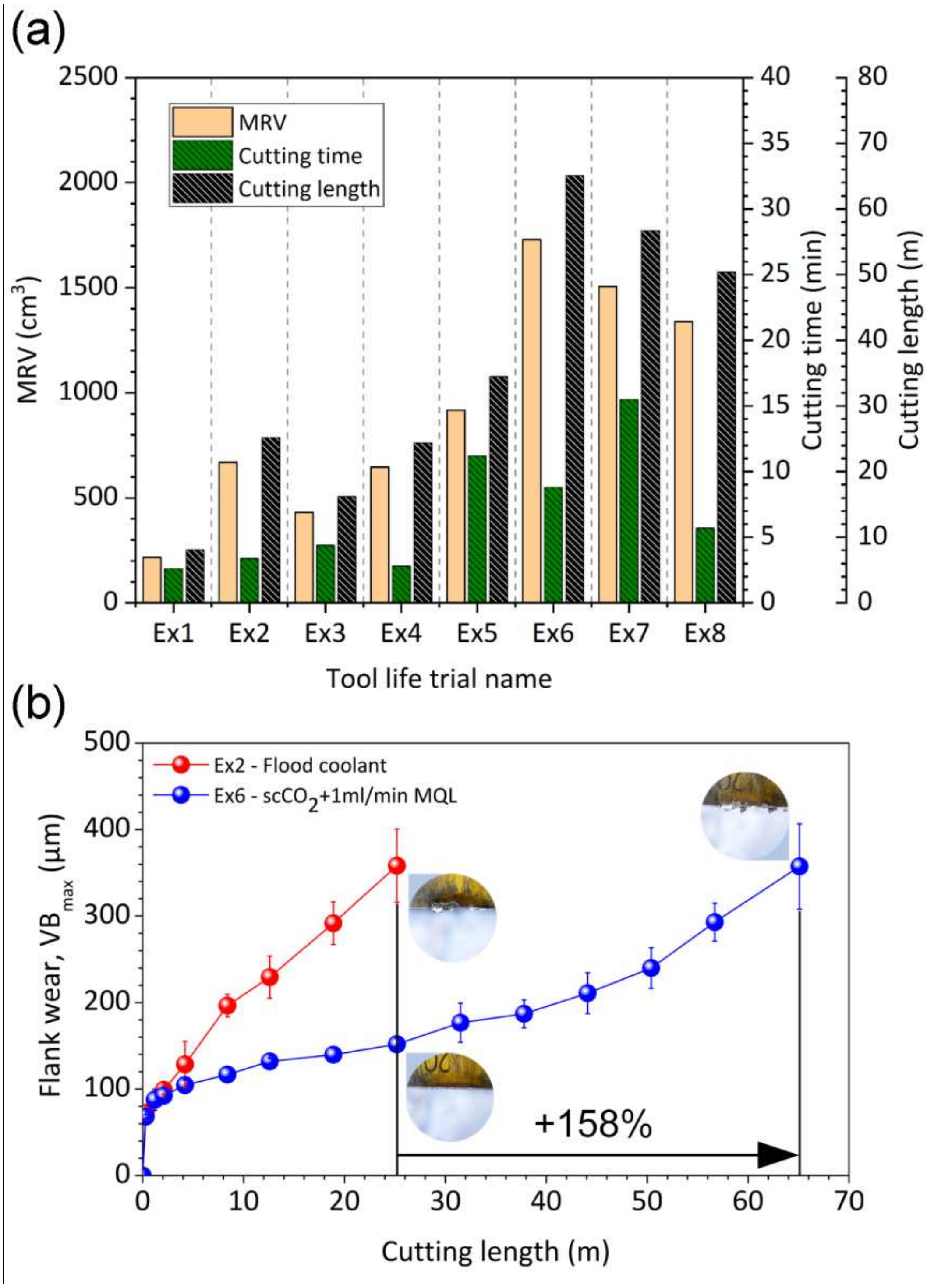

Fig. 4. (a) Impact of various cutting conditions on tool life in terms of cutting length and time with material removed volume (MRV) in milling with $scCO_2$+MQL and flood coolant. In (b), the maximum flank wear (VB_{max}) values in comparison to cutting length.

Fig. 4(b) shows the flank wear progression with the cutting length. Based on above discussion and from the graph presented in Fig. 4, it can be concluded that the highest volume of material removed is achieved in milling with $scCO_2$ at higher feed rate when the cutting speed is 215 m/min. The lower cutting speed, however, may cause an increase in amplitude of tool vibration and friction on the tool-chip interface, which resulted in the progressive increase of flank wear [29]. At these cutting conditions, the tool life is 8.77 min whereas the mean flank wear value was about 360 μm. The tool life was almost two times smaller, in comparison to milling at lower feed rate with an increased cutting speed where the tool life was 15.46 min and the average flank wear value at the end point was about 320 μm.

3.2 Surface roughness and microhardness

Fig. 5 shows a topography of machined surfaces scanned using confocal laser scanning microscopy on the horizontal line with a constant slope in the feed direction.

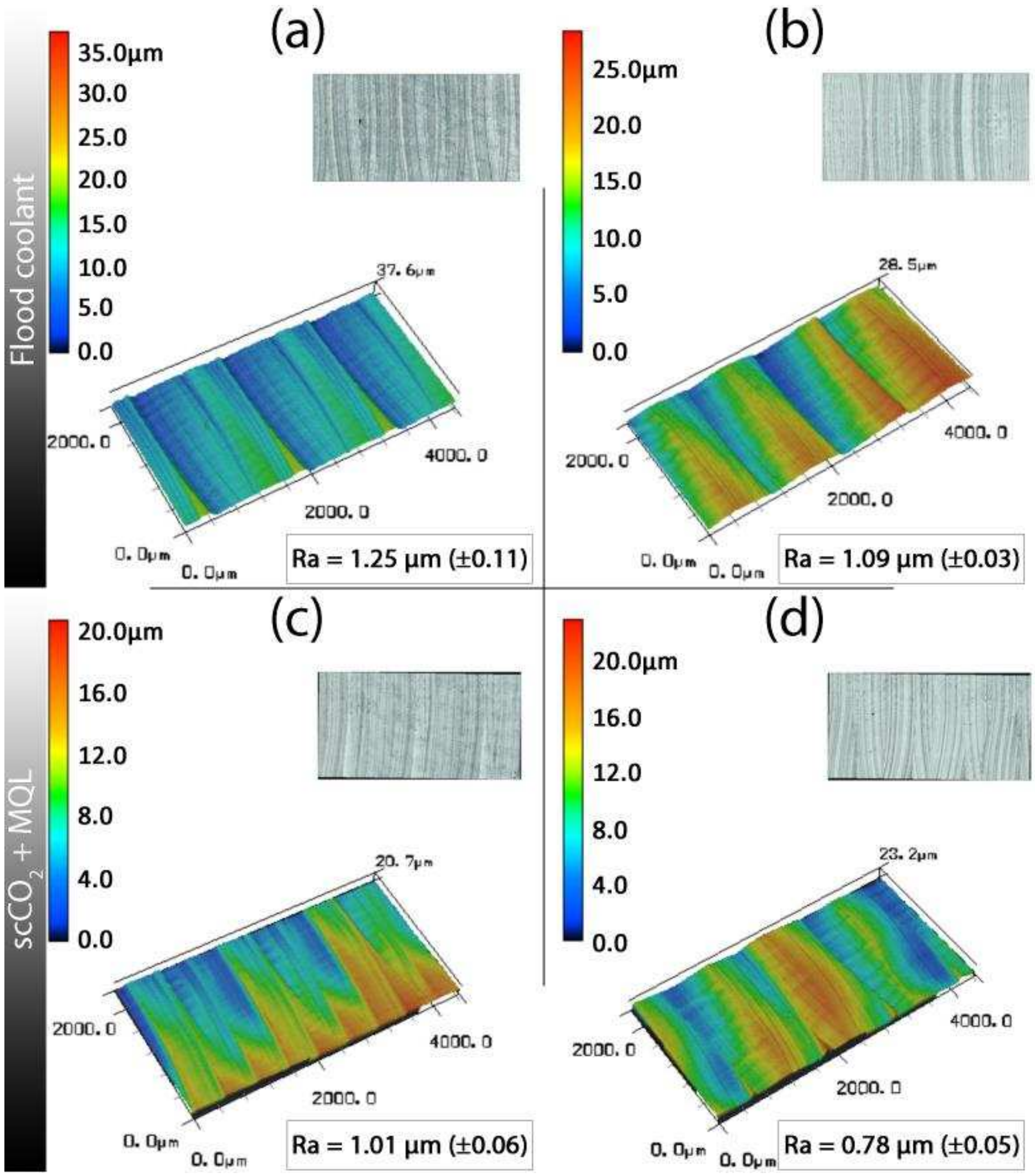

Fig. 5. 3D models of surface topography with corresponding confocal images of the machined surfaces at constant speed of 215 m/min under (a, b) flood and (c, d) $scCO_2$+MQL cooling conditions and f_z (a, c) 0.5 mm/tooth and (b, d) 1.20 mm/tooth.

The mean surface roughness value from each sample was calculated based on six measurements obtained from the surface profile. It can be seen in Fig. 5 that with an increase in feed rate from 0.50 mm/tooth to 1.20 mm/tooth, the Ra values were decreasing. This was seen for both cooling methods (flood coolant and $scCO_2$+MQL). Typically, as seen in literature, the relationship between feed rate and surface roughness was such that the surface roughness increases with increasing feed rate, as higher feed rate results in higher cutting temperature and increased flank wear [30, 31]. The highest surface roughness was expected with a higher feed rate because of increased friction between the tool and the workpiece. However, an increase in the feed rate from 0.50 mm/tooth to 1.20 mm/tooth resulted in reduced surface roughness by around 12.8% and 22.8% in milling with flood coolant and $scCO_2$+MQL, respectively. Similar trend was observed by Liu et al. [32] due to the increased plastic flow at lower feed rates which was caused by strain gradient-induced strengthening of the workpiece material at a direction opposite to the feed direction. The plastic deformation ahead of the tool tends to form the machined surface as it also depends on the cutting tool edge geometry [33]. Further investigation revealed that the surface roughness increases with increasing cutting speed. The surface roughness value increased from ~0.78 μm to ~0.85 μm in milling with $scCO_2$ at constant feed rate of 1.20 mm/tooth where the cutting speed varied from 215 m/min to 255 m/min, respectively (all results not shown here). A similar trend was observed when milling with flood coolant at lower feed rate. The surface roughness value increased rapidly about 19% in milling with flood coolant at higher cutting speed. The reason for this increase in surface roughness at higher cutting speed can be attributed to the formation of a built-up-edge (BUE), which is formed as a result of shear stress on the leading surface of the workpiece that adheres the workpiece material to the edge of the tool, causing surface scratching and effectively changing the cutter geometry. Therefore, it needs to be highlighted that finding the right relationship between the feed rate and the surface roughness is very important, since it affects the surface finish. Furthermore, it can be seen in Fig. 5 that the surface roughness value is lower when milling with the $scCO_2$ as compared to flood coolant. At higher feed rates, the surface roughness is 0.78 μm in milling with the $scCO_2$ cooling, which translates into about 40% surface finish improvement in comparison to flood coolant. The higher surface roughness when milling with flood coolant could result from the higher specific cutting energy which arises from increased workpiece strength due to strain gradient and temperature effects. This also affects the microstructure within the near-surface region of the workpiece. Fig. 6 shows the microstructure of the cross-sections below the machined surfaces of the samples machined with different feed rates but at the same cutting speed.

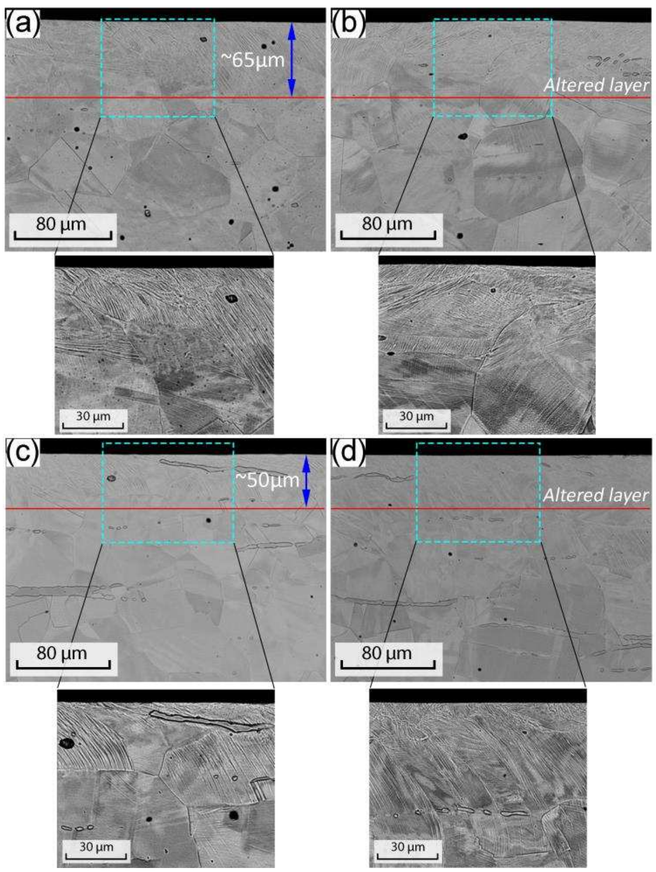

Fig. 6. SEM images of the workpiece machined surface layer at V_c = 215 m/min and the feed rate (a, c) 0.50 mm/tooth and (b, d) 1.20 mm/tooth upon cooling with (a, b) flood coolant and (c, d) $scCO_2$+ MQL. Insets show the area marked with a frame at higher magnification (2500x).

From Fig. 6(a, b) it can be seen that deeper microstructure alterations are induced by milling with flood coolant at f_z = 0.50 mm/tooth and 1.20 mm/tooth (V_c = 215 m/min). The effect of subsurface alterations on the workpiece surface microhardness is shown in Fig. 7.

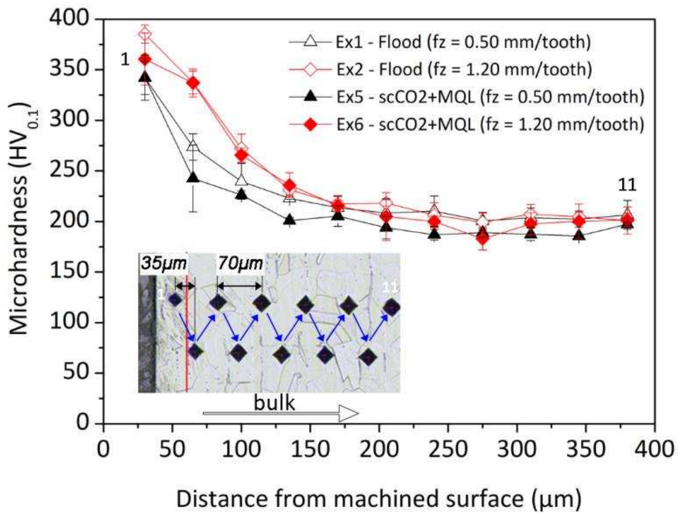

Fig. 7. Microhardness (μHV) depth profiles obtained for the machined surface layer with flood coolant and $scCO_2$+MQL (V_c = 215 m/min).

To estimate the modified surface layer thickness, the hardness values were compared and related to the microstructure. A layer thickness strongly altered by plastic deformation was estimated to be in a range from 50 to 65 μm (Fig. 6). At higher temperatures, grain boundary sliding takes the dominant role in plastic deformation, and dislocation movement is also easier compared to milling at very low temperatures [34]. Therefore, the grain boundaries in milling with the $scCO_2$ act as strong obstacles which tend to slow down the movement of dislocations, which consequently results in smaller thickness values of the altered surface layer as compared to the flood coolant. Further, it can be seen from the graph presented in Fig. 7 that the surface microhardness increases with increasing feed rate for both flood coolant and $scCO_2$+MQL cooling methods. A higher microhardness value at the feed rate of 1.20 mm/tooth results from the increased shear strain rate for higher feed rates causing the strain hardening to increase, and consequently leading to a significant increase in microhardness [35]. The mean microhardness value is about 340HV for both flood coolant and scCO_2 at the feed rate of 0.50 mm/tooth. Further increase in the feed rate up to 1.20 mm/tooth at the same cutting speed (V_c = 215 m/min) caused an increase in microhardness up to 385 HV and 360 HV when milling is carried out with flood coolant and scCO_2, respectively. It can be reported that there is no apparent difference in the surface microhardness between milling with flood coolant and scCO_2+MQL (Fig. 7).

3.3 Residual stresses in the machined surfaces

The residual stresses were measured on plates, machined during the DoE stage of experiments, in the transverse (φ = 0°) and longitudinal (φ = 90°) directions. Fig. 8 shows the regression coefficient of the residual stress model for milling austenitic stainless steel 304L with flood coolant [Fig. 8(a) and scCO_2+MQL Fig. 8(b)].

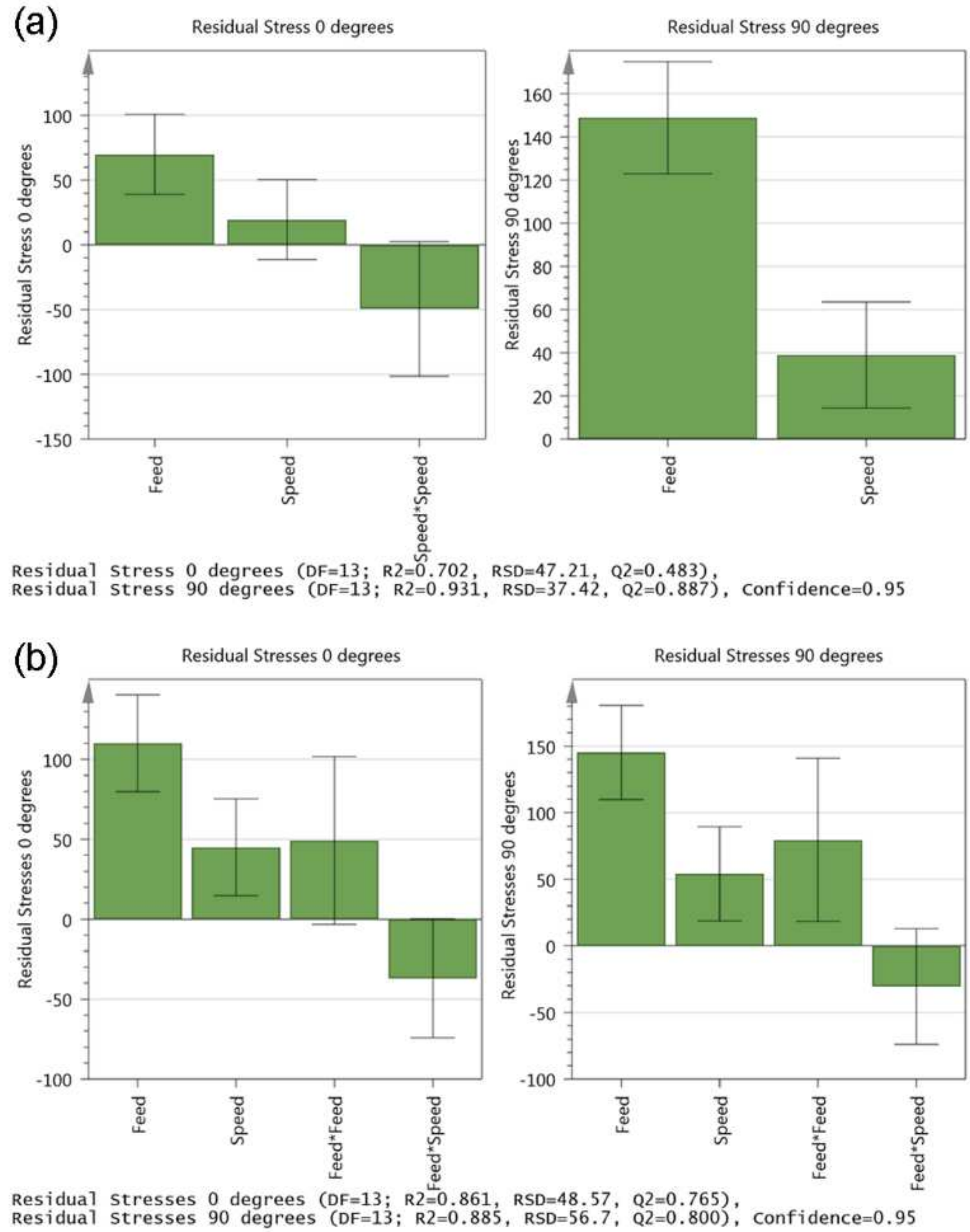

Fig. 8. Regression coefficient plot for the influence of variables on residual stress in 0° and 90° directions in milling of stainless steel 304L with (a) flood coolant and (b) $scCO_2$+MQL.

As can be seen in Fig. 8, such factors as feed rate and cutting speed had a positive effect on the response in both cases. This implies that with an increase of feed rate and cutting speed, the value of measured residual stress is also increasing. In Fig. 8, the error bars were confidence intervals and indicated the size of the noise in the experiment. The R^2 and Q^2 values were calculated for the Multiple Linear Regression (MLR) model at the confidence level of 95%.

The R^2 and Q^2 values for residual stress in the transverse ($\varphi = 0°$) direction, while milling with flood coolant, were 0.702 and 0.483, respectively, whereas for residual stress in 90° direction were 0.931 and 0.887, respectively, at the 95% confidence level. Similarly, the corresponding values of 0.861 (R^2) and 0.765 (Q^2) were obtained for residual stress in 0° direction, while milling with scCO_2 and MQL (R^2 and Q^2 equals to 0.885 and 0.861 in 90° direction, respectively).

The size of the regression coefficient indicates the significance of a particular factor in a model. Its size corresponds to the change in a response when a factor varies from low to high level, while the other factors are kept at their average values. It was observed that the strongest term affecting the residual stress is feed rate.

Fig. 9 presents a 2D response surface contour plots for mean residual stresses in the transverse (φ = 0°) and longitudinal (φ = 90°) directions.

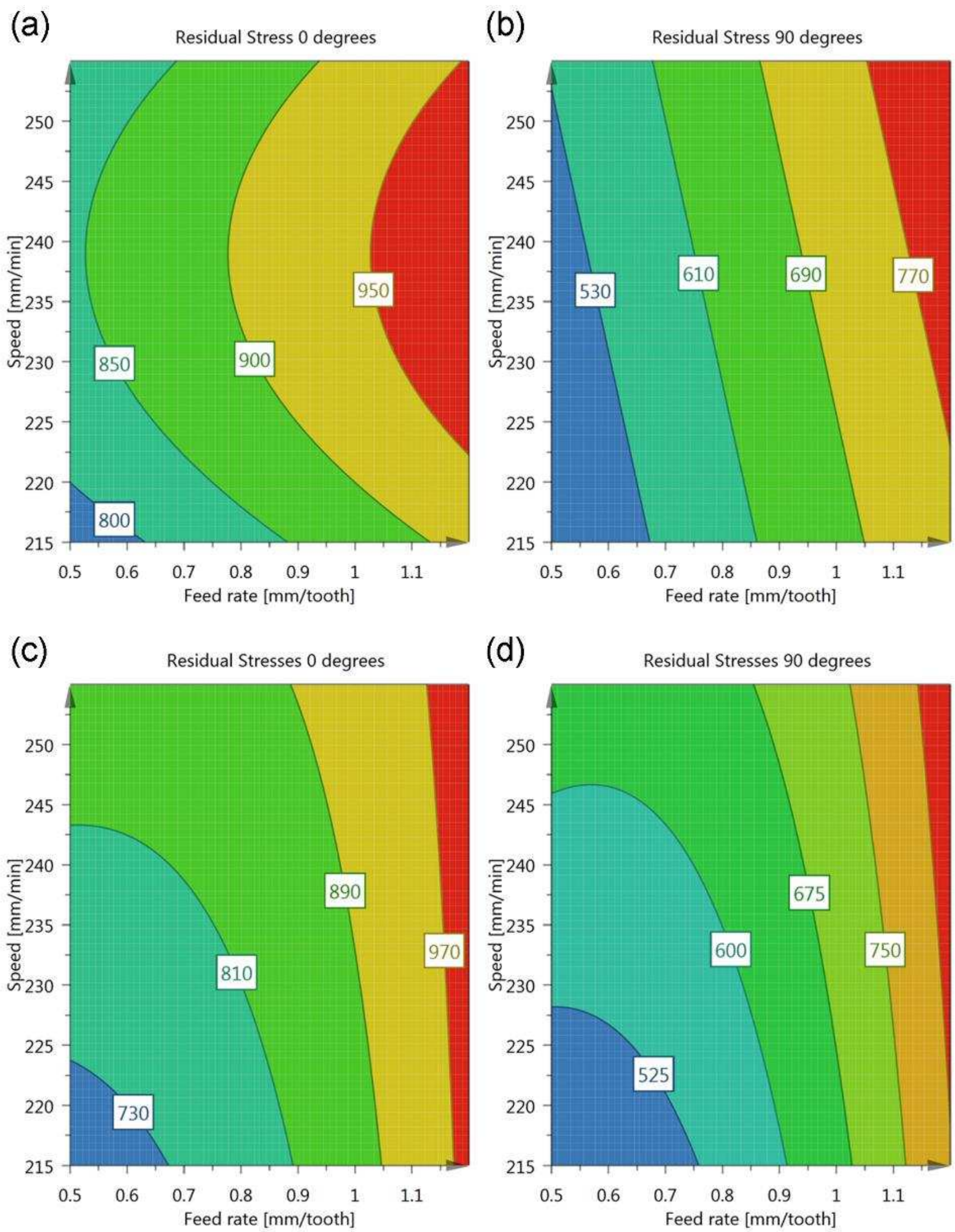

Fig. 9. 2D response contour plot of mean residual stresses in relation between feed rate and cutting speed in milling with (a, b) flood coolant and (c, d) $scCO_2$ with MQL.

The 2D contour plots present the predicted response values based on a specified regression model for particular responses spanned by two factors (feed rate per tooth and cutting speed). The residual stresses measured on workpiece surface were tensile in milling with both flood coolant and $scCO_2$+MQL, which can also be seen in Fig. 9. The formation of surface tensile residual stress can be related to the heat flow rate and temperature changes in machining [36]. As previously noted, the surface microhardness obtained from the same assessed locations of machined workpiece with $scCO_2$+MQL did not change significantly compared to flood coolant. Thus, it can be assumed that no hardening work had occurred during the DoE stage in milling experiments. The faster cooling rate in milling with $scCO_2$+MQL resulted in slightly higher tensile stresses on the workpiece surface compared with flood coolant, however, no significant difference in residual stress were observed. As mentioned previously, feed rate had the strongest influence on tensile residual stress values. The increase in feed rate results in the increased relative movement of the workpiece and cutting tool. This in turn decreases the material removal rate efficiency, and consequently gains higher residual stress [37].

Additional experiments were designed and conducted to validate the mean residual stress model for milling with both cooling methods. The validation experiments were conducted at V_c = 245 m/min and f_z = 0.7 mm/tooth. The predicted value of residual stress in the transverse (φ = 0°) direction in workpiece surface, while milling with flood coolant was 880.07 MPa, giving an error of 2.77% compared to the experimental value (855.67 MPa). In turn, the predicted value of residual stress in the longitudinal (φ = 90°) direction in workpiece surface was 600.14 MPa, giving an error of 8.40% compared to the experimental value (650.57 MPa). Further, the predicted value of residual stress in the transverse (φ = 0°) direction in workpiece surface after milling with $scCO_2$ and MQL was 829.13 MPa, giving an error of 3.34% compared to the experimental value (856.80 MPa), and in the longitudinal (φ = 90°) direction the corresponding values of 605.50 MPa and 649.90 MPa were measured with an error of 7.34%.

The validation model results showed very good prediction power of the mean residual stress in the transverse and longitudinal directions. No statistically significant models were built in terms of surface roughness and microhardness.

4 Summary and conclusions

In this paper, the DoE experiments with tool life trials were conducted to study the influence of cutting parameters (speed and feed rate at constant depth of cut) on responses during milling process of austenitic stainless steel 304L under different cooling methods (flood coolant vs. scCO_2 with MQL). Based on experimental results, the following conclusions were drawn:

1) The maximum increase in tool life was seen at V_c = 215 m/min and f_z = 0.50 mm/tooth, where the cutting time varied from 2.63 min for flood coolant to 11.16 min using scCO_2 with MQL (increase in tool life of ~324%).
2) The maximum MRV achieved during milling with scCO_2+MQL was 1729 cm^3 which is a ~158% increase in comparison to flood coolant (at higher feed of 1.20 mm/tooth and cutting speed of 215 m/min).
3) For higher cutting parameters (f_z = 1.20 mm/tooth and V_c = 255 m/min), an increase in tool life (~106%) was reported during milling with the scCO_2+MQL in comparison to flood coolant.
4) The surface roughness values decreased with increasing feed rate. About 30% decrease in surface roughness was observed after milling with scCO_2+MQL at higher feed rate and lower cutting speed of 215 m/min. Generally, an increase in surface roughness was

observed with increasing cutting speed. This was most likely a result of a built-up-edge (BUE) formation. It can be concluded that $scCO_2$ indicates a trend to create a surface finish with lower Ra value. This will be investigated as part of a further study.

5) No significant microstructural changes were observed in stainless steel 304L after milling the workpiece with $scCO_2$+MQL when compared to flood coolant. However, the analysis of surface layer alterations showed a slight increase in thickness of the affected layer after milling with flood coolant.
6) No apparent changes in the surface microhardness were observed between milling with flood coolant and $scCO_2$+MQL. The increase in microhardness with increasing feed rate was observed as a result of increase in strain hardening in both cooling methods.
7) The tensile residual stresses were induced in the workpiece surface during milling with both flood coolant and $scCO_2$+MQL, results were comparable for both coolant methods. The residual stress values predicted by the model obtained from the DoE stage of experiments were consistent with the experimental values. The feed rate was found to be the most influential factor affecting the residual stress values.

Acknowledgements

Authors would like to acknowledge financial support from the High Value Manufacturing Catapult (HVMC), UK.

References

[1] I.S. Jawahir, E. Brinksmeier, R.M'Saoubi, D.K. Aspinwall, J.C. Outeiro, D. Meyer, D. Umbrello, A.D. Jayal, Surface integrity in material removal processes: Recent advances, CIRP Annals – Manufacturing Technology 60 (2011) 603–626.

[2] S. Debnath, M.M. Reddy, Q.S. Yi, Environmental friendly cutting fluids and cooling techniques in machining: a review, Journal of Cleaner Production 83 (2014) 33–47.

[3] A. Shokrani, V. Dhokia, S.T. Newman, Environmentally conscious machining of difficult-to-machine materials with regard to cutting fluids, International Journal of Machine Tools & Manufacture 57 (2012) 83–101.

[4] Y. Yildiz, M. Nalbant, A review of cryogenic cooling in machining processes, International Journal of Machine Tools & Manufacture 48 (2008) 947–964.

[5] T. Mulyana, E. Abd Rahim, S.N. Md Yahaya, The influence of cryogenic supercritical carbon dioxide cooling on tool wear during machining high thermal conductivity steel, Journal of Cleaner Production 164 (2017) 950–962.

[6] A. Ahmad-Yazid, Z. Taha, I.P. Almanar, A review of cryogenic cooling in high speed machining (HSM) of mold and die steels, Scientific Research and Essays 5 (2010) 412–427.

[7] I.S. Jawahir, H. Attia, D. Biermann, J. Duflou, F. Klocke, D. Meyer, S.T. Newman, F. Pusavec, M. Putz, J. Rech, V. Schulze, D. Umbrello, Cryogenic manufacturing processes, CIRP Annals – Manufacturing Technology 65 (2016) 713–736.

[8] N. Tapoglou, M.I. Aceves Lopez, I. Cook, Ch.M. Taylor, Investigation of the influence of CO_2 cryogenic coolant application on tool wear, Procedia CIRP 63 (2017) 745–749.

[9] A.A. Khan, M.I. Ahmed, Improving tool life using cryogenic cooling, Journal of Materials Processing Technology 196 (2008) 149–154.

[10] S.G. Acharyya, A. Khandelwal, V. Kain, A. Kumar, I. Samajdar, Surface working of 304L stainless steel: Impact on microstructure, electrochemical behavior and SCC resistance, Materials Characterization 72 (2012) 68–76.

[11] P.S. Kumar, S.G. Acharyya, S.V. Ramana Rao, K. Kapoor, Distinguishing effect of buffing vs. grinding, milling and turning operations on the chloride induced SCC susceptibility of 304L austenitic stainless steel, Materials Science & Engineering A 687 (2017) 193–199.

[12] T. Allen, J. Busby, M. Meyer, D. Petti, Materials challenges for nuclear systems, Materials Today 12, 13 (2010) 14–23.

[13] M. Kaladhar, Machining of austenitic stainless steel – a review, International Journal of Machining and Machinability of Materials 12 (2012) 178–192.

[14] A.K. Sharma, A.K. Tiwari, A.R. Dixit, Effects of Minimum Quantity Lubrication (MQL) in machining processes using conventional and nanofluid based cutting fluids: A comprehensive review, Journal of Cleaner Production 127 (2016) 1–18.

[15] Sandvik Coromant, How to apply coolant and cutting fluid in turning. https://www.sandvik.coromant.com/en-gb/knowledge/general-turning/pages/how-to-apply-coolant-and-cutting-fluid-in-turning.aspx.

[16] N. King, L. Keranen, K. Gunter, J.W. Sutherland, Wet versus dry turning: a comparison of machining costs, product quality, and aerosol formation, SAE 2001 World Congress. ISSN 0148-7191.

[17] M. Nalbant, Y. Yildiz, Effect of cryogenic cooling in milling process of AISI 304 stainless steel, Trans. Nonferrous Met. Soc. China 21 (2011) 72–79.

[18] N. Hanenkamp, S. Amon, D. Gross, Hybrid supply system for conventional and CO_2/MQL-based cryogenic cooling, Procedia CIRP 00 (2018) 000–000.

[19] O. Pereira, P. Català, A. Rodríguez, T. Ostra, J. Vivancos, A. Rivero, L.N. López de Lacalle, The use of hybrid CO_2+MQL in machining operations, Procedia Engineering 132 (2015) 492–499.

[20] O. Pereira, A. Rodríguez, A.I. Fernánded-Abia, J. Barreiro, L.N. López de Lacalle, Cryogenic and minimum quantity lubrication for an eco-efficiency turning of AISI 304, Journal of Cleaner Production 139 (2016) 440–449.

[21] B.D. Jerold, M.P. Kumar, Experimental comparison of carbon-dioxide and liquid nitrogen cryogenic coolants in turning of AISI 1045 steel, Cryogenics 52 (2012) 569–574.

[22] T. Lu, O.W. Dillon, Jr., I.S. Jawahir, A thermal analysis framework for cryogenic machining and its contribution to product and process sustainability, Proceedings of the 11th (2013) Global Conference on Sustainable Manufacturing - Innovative Solutions. ISBN 978-3-7983-2609-5.

[23] P. Freund, S. Bachu, D. Simbeck, K. Thambimuthu, M. Gupta, Properties of CO_2 and carbon-based fuels, in: B. Metz, O. Davidson, H. de Coninck (Eds.), IPCC Special report on carbon dioxide capture and storage, Cambridge University Press, New York, 2005, pp. 383–400.

[24] L. Eriksson, E. Johansson, N. Kettaneh-Wold, C. Wikstrom, S. Wold, Design of Experiments - Principles and Applications (2008) MKS Umetrics AB.

[25] ISO 8688-1:1989, Tool life testing in milling Part 1 – face milling, International Organisation for Standardisation, Geneva, 1989.

[26] R. Unnikrishnan, K.S.N. Satish Idury, T.P. Ismail, A. Bhadauria, S.K. Shekhawat, R.K. Khatirkar, S.G. Sapate, Effect of heat input on the microstructure, residual stresses and corrosion resistance of 304L austenitic stainless steel weldments, Materials Characterization 93 (2014) 10–23.

[27] ISO 4287:1997, Geometrical Product Specifications (GPS) -- Surface texture: Profile method -- Terms, definitions and surface texture parameters, International Organisation for Standardisation, Geneva, 1997.

[28] M.A. Ince, İ. Asiltürk, Effects of cutting tool parameters on vibration, 2016 3rd International Conference on Mechanics and Mechatronics Research (ICMMR 2016).

[29] A. Siddhpura, R. Paurobally, A study of the effects of friction on flank wear and the role of friction in tool wear monitoring, Australian Journal of Mechanical Engineering 10 (2012) 141–156.

[30] T. Özel, Y. Karpat, L. Figueira, J.P. Davim, Modelling of surface finish and tool flank wear in turning of AISI D2 steel with ceramic wiper inserts, Journal of Materials Processing Technology 189 (2007) 192–198.

[31] A.A. Khan, A.K.M. Mohiuddin, N.H. Norhamzan, A comparative study on flank wear of ceramic and tungsten carbide inserts during high speed machining of stainless steel, International Journal of Applied Engineering Research 13 (2018) 2541–2544.

[32] K. Liu, S.N. Melkote, Effect of plastic side flow on surface roughness in micro-turning process, International Journal of Machine Tools & Manufacture 46 (2006) 1778–1785.

[33] F. Xu, F. Fang, X. Zhang, Side flow effect on surface generation in nano cutting, Nanoscale Research Letters 12:359 (2017) 1–12.

[34] Y. Kaynak, T. Lu, I.S. Jawahir, Cryogenic machining-induced surface integrity: A review and comparison with dry, MQL, and flood-cooled machining, Machining Science and Technology: An International Journal 18:2 (2014) 149–198.

[35] H. Senussi, Interaction effect of feed Rate and cutting speed in CNC-turning on chip micro-hardness of 304-austenitic stainless steel, International Journal of Mechanical, Aerospace, Industrial, Mechatronic and Manufacturing Engineering 1 (2007) 159–164.

[36] J.P. Davim (Ed.), Surface integrity in machining, Springer, Berlin (2010).

[37] A. Reimer, X. Luo, Prediction of residual stress in precision milling of AISI H13 steel, Procedia CIRP 71 (2018) 329–334.